Acta Mech 229, 2967–2977 (2018)
https://doi.org/10.1007/s00707-018-2155-x

ORIGINAL PAPER

Chunlong Gu · Peng Li · Feng Jin · Gongfa Chen · Liansheng Ma

Effects of the imperfect interface and viscoelastic loading on vibration characteristics of a quartz crystal microbalance

Received: 17 March 2017 / Revised: 15 March 2018 / Published online: 12 April 2018

Abstract The interfacial adhesion and viscoelasticity of an additional mass layer have a significant influence on the resonant frequency of a quartz crystal microbalance (QCM), especially when the attached mass layer is thick. In this study, a detailed quantitative investigation is conducted on the influence of the interface parameter and viscosity coefficient on the resonant frequency and admittance of a QCM. The obtained explicit expression of free vibration of the QCM can be numerically solved using Muller's method. The results obtained in this study show that the viscoelasticity of the mass layer and its bonding characteristics significantly affect the performances of the QCM, such as the resonance frequency, displacement, and stress distributions, and the peak and bandwidth of admittance. The non-proportional relation between the resonance frequency and thickness of the mass layer becomes obvious when the thickness of the mass layer is larger than 2% that of the quartz plate. Meanwhile, the error between the exact solution and Sauerbrey's solution is enlarged as the interface parameter increases or the viscosity coefficient decreases. The proposed method will be more precise in solving the resonant frequency than Sauerbrey's equation does and able to provide a guidance for determining the viscosity of an attached mass layer. The novel points in the article are as follows: (i) The effects of the imperfect interface and viscosity on the resonance frequency of a QCM at different layer thicknesses are investigated. (ii) The difference between effects of the imperfect interface and viscosity on the characteristics of the admittance is discussed in detail.

1 Introduction

Quartz crystal has been used in numerous acoustic wave devices, such as resonators, oscillators, filters, and QCMs, because of its good temperature stability. A QCM, whose basic structure consists of a quartz crystal plate with two electrodes bonded on the two sides of the plate, is a very sensitive device for the detection of mass, measurement of film thickness, and component analysis of gases or liquids. Using a QCM, the physical

C. Gu · G. Chen (✉)
School of Civil and Transportation Engineering, Guangdong University of Technology, Guangzhou 510006, People's Republic of China
E-mail: gongfa.chen@gdut.edu.cn

P. Li
School of Human Settlements and Civil Engineering, Xi'an Jiaotong University, Xi'an 710049, People's Republic of China

F. Jin
State Key Laboratory for Strength and Vibration of Mechanical Structures, School of Aerospace, Xi'an Jiaotong University, Xi'an 710049, People's Republic of China

L. Ma
School of Science, Lanzhou University of Technology, Lanzhou 730050, People's Republic of China

characteristics of the attached mass layer such as density, thickness, and stiffness can be determined from the frequency variation [1].

Attracted by its promising applications, many researchers have been engaged in improving the performance of QCMs. Sauerbrey [2] reported a linear relationship between the variation of the resonance frequency of an oscillating quartz crystal and the additional mass. This relationship is referred to as Sauerbrey's equation. Subsequent studies have indicated that the effect of mass loading outside the electrode area on the resonant frequency of a QCM must be considered [3]. Kong et al. [4] discussed the effect of a partial mass layer on the properties of QCM and found that the trapped modes were sensitive to the mass layer. More fundamental studies have been conducted recently on the behaviors of QCMs [5–7].

The above-mentioned studies are all based on the assumption that no energy is dissipated in the additional mass layer. However, QCM technique is usually used to characterize the properties of liquids [8] and viscoelastic polymer films [9,10], where energy loss is inevitable because of the damping effect. Numerous studies have been conducted on the characteristics of QCMs with respect to energy dissipation. For example, the frequency shift of a quartz crystal resonator caused by Newtonian liquid was determined in [11]. Furthermore, the effects of elastic and viscoelastic mass layers were theoretically investigated in [12]. The influence of fluid viscosity on the cutoff frequency can be indirectly identified using the thickness-shear mode [13]. Arnau et al. [14] analyzed a quartz crystal resonator based on the thickness-shear mode in a semi-infinite viscoelastic medium using an extended Butterworth–Van Dyke model. The material parameters [15], e.g., admittance and impedance of QCMs, were experimentally determined for detecting additional liquid layers [16].

A perfect interface was assumed between the mass layer and the quartz crystal plate in the studies mentioned above. However, an imperfect bond is inevitable because of various factors such as microcracks, temperature mismatch, corrosion, and flow. It is well known that Sauerbrey's equation gives inaccurate results due to the inhomogeneity of mass and amplitude of vibration distributions [17] or slip interfaces [18,19]. Considering these limitations, we study the effect of an imperfect interface and viscoelastic mass layer on the properties of QCMs. In contrast to previous research, both the inertial and stiffness effects of the viscoelastic mass layer are considered in free and forced vibrations, and the frequency shift caused by the additional mass layer has been calculated from our theoretical formula.

2 Theoretical analysis

The structure of a QCM comprises an AT-cut quartz crystal plate and a viscoelastic mass layer (Fig. 1). Its thickness direction is along the y-axis, and the z-axis is perpendicular to the x–y plane. The viscoelastic mass layer with thickness h_2 is imperfectly attached to the quartz crystal plate of thickness h_1. Two electrodes are present at the two surfaces of the quartz crystal plate. The periodic voltage $\pm V_0 \exp(i\omega t)$ is simultaneously applied to the electrodes. The electrodes are very thin compared with the additional mass layer; thus, their mass and inertia are neglected [20].

When an electrical field is applied across the quartz crystal plate along the y-direction, a thickness-shear mode can be generated in the lateral direction; the corresponding wave equation in the plane strain problem can be expressed in the following form [21]:

$$\begin{cases} \bar{c}_{66}\dfrac{\partial^2 u_1}{\partial y^2} = \rho_1 \dfrac{\partial^2 u_1}{\partial t^2}, \\ e_{26}\dfrac{\partial^2 u_1}{\partial y^2} - \varepsilon_{22}\dfrac{\partial^2 \varphi_1}{\partial y^2} = 0 \end{cases} \tag{1}$$

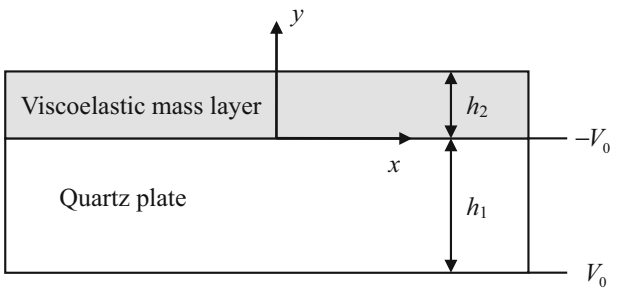

Fig. 1 AT-cut quartz plate with viscoelastic mass layer

where u_1 and φ_1 denote the mechanical displacement and electric potential function in the x-direction of the quartz crystal plate, respectively, and ρ_1 is the mass density; $\bar{c}_{66}$, e_{26}, and ε_{22} are the effective elastic shear modulus, the piezoelectric and dielectric constants of the quartz crystal, respectively. The effective elastic shear modulus can be expressed as $\bar{c}_{66} = c_{66} + i\omega\eta_q + \frac{e_{26}^2}{\varepsilon_{22}}$, where c_{66}, ω, and η_q denote the elastic constant, angular frequency, and viscosity coefficient of the quartz crystal, and $i = \sqrt{-1}$.

Similarly, the equation of motion of the viscoelastic layer is [12]:

$$\bar{\mu}\frac{\partial^2 u_2}{\partial y^2} = \rho_2 \frac{\partial^2 u_2}{\partial t^2} \tag{2}$$

where u_2 and ρ_2 are the mechanical displacement in the x-direction and the density of the viscoelastic mass layer, respectively, and $\bar{\mu} = \mu + i\omega\eta$ is the effective elastic shear modulus. Here, μ and η are the elastic constant and the viscosity coefficient of the mass layer, respectively.

The solutions of Eq. (1) can be easily derived as follows [21]:

$$u_1(y,t) = [A_1 \cos(k_1 y) + B_1 \sin(k_1 y)]\, \mathrm{e}^{i\omega t}, \tag{3.1}$$

$$\varphi_1(y,t) = \left[\frac{e_{26}}{\varepsilon_{22}} A_1 \cos(k_1 y) + \frac{e_{26}}{\varepsilon_{22}} B_1 \sin(k_1 y) + C_1 y + D_1\right] \mathrm{e}^{i\omega t}, \tag{3.2}$$

and the shear stress can be expressed as

$$\begin{aligned}\sigma_{yx}^{(1)}(y,t) &= \left(c_{66} + i\omega\eta_q\right)\frac{\partial u_1}{\partial y} + e_{26}\frac{\partial \varphi_1}{\partial y} \\ &= \{\bar{c}_{66} k_1 [-A_1 \sin(k_1 y) + B_1 \cos(k_1 y)] + e_{26} C_1\}\, \mathrm{e}^{i\omega t}\end{aligned} \tag{4}$$

where A_1, B_1, C_1, and D_1 are constants to be determined, and $k_1 = \omega\sqrt{\frac{\rho_1}{\bar{c}_{66}}}$ is the wavenumber of the thickness-shear mode in the quartz crystal plate.

Similarly, the solution of Eq. (2) can be written as

$$u_2(y,t) = [A_2 \cos(k_2 y) + B_2 \sin(k_2 y)]\, \mathrm{e}^{i\omega t}, \tag{5}$$

and the shear stress can be expressed as

$$\sigma_{yx}^{(2)}(y,t) = \bar{\mu}\frac{\partial u_2}{\partial y} = \{\bar{\mu} k_2 [-A_2 \sin(k_2 y) + B_2 \cos(k_2 y)]\}\, \mathrm{e}^{i\omega t} \tag{6}$$

where A_2 and B_2 are constants to be determined, and $k_2 = \omega\sqrt{\frac{\rho_2}{\bar{\mu}}}$ is the corresponding wavenumber within the viscoelastic mass layer. The six unknown constants can be determined from boundary conditions. Six independent boundary conditions are required to describe the physical behavior of quartz and the viscoelastic layer. The wave displacement generates an accompanying electrical potential through which the piezoelectric wave can be electrically detected. The impedance/admittance analysis, in which the spectra of impedance and admittance are recorded as functions of the excitation frequency, is widely used to detect the perturbation of bulk acoustic wave (BAW) sensors. The admittance is defined as the ratio of the input current to voltage. The current across the quartz crystal, which is the time derivative of the charge, can be expressed as [21]

$$I = -i\omega\varepsilon_{22} C_1 S \tag{7}$$

where S is the effective electrode surface area and C_1 is the constant from Eq. (3.2). The admittance of the quartz crystal resonator can be given as

$$Y = \frac{I}{V} = \frac{-i\omega\varepsilon_{22} S}{2V_0} C_1 = G + iB \tag{8}$$

where G is the conductance and B is the susceptance. The magnitude [$|Y|$] and phase angle (θ) of admittance can be expressed as [18]

$$|Y| = (G^2 + B^2)^{1/2}, \tag{9}$$

$$\theta = \tan^{-1}\left(\frac{B}{G}\right). \tag{10}$$

The impedance is $Z = \frac{V}{I} = R + iX$, where R and X denote the resistance and reactance, respectively [22].

The mechanical and electrical boundary and continuity conditions must be satisfied for the problem. For the electrode and the traction-free surfaces, the stress component and electric potential function are given as follows:

$$\sigma_{yx}^{(1)}(-h_1, t) = 0, \quad \sigma_{yx}^{(2)}(h_2, t) = 0. \tag{11}$$

$$\varphi_1(-h_1, t) = V_0, \quad \varphi_2(0, t) = -V_0. \tag{12}$$

When the viscoelastic layer is imperfectly bonded to the surface of the AT-cut quartz crystal plate, the shear-lag model, which has been verified experimentally, can be used to describe the mechanical behaviors of the imperfect interface [23,24]. The interface is then treated as a layer with no thickness. However, it still possesses elasticity and elastic strain energy, i.e., the shear displacement across the interface can be different to account for its deformation [18,19,23,24]. Namely,

$$\sigma_{yx}^{(1)}(y, t) = \sigma_{yx}^{(2)}(y, t) = K\left[u_2(0, t) - u_1(0, t)\right], \tag{13}$$

where K represents the elastic constant of the interface. When $K \to 0$, the two materials lose their mechanical interaction, whereas if $K \to +\infty$, the two layers are attached perfectly. Substitution of Eqs. (3–6) into Eqs. (11–13) yields the following six linear and homogeneous equations for coefficients A_1, B_1, C_1, D_1, A_2, and B_2:

$$\begin{cases} \bar{c}_{66}k_1\left[A_1\sin(k_1h_1) + B_1\cos(k_1h_1)\right] + e_{26}C_1 = 0, \\ \frac{e_{26}}{\varepsilon_{22}}\left[A_1\cos(k_1h_1) - B_1\sin(k_1h_1)\right] - C_1h_1 + D_1 = V_0, \\ \bar{\mu}k_2\left[-A_2\sin(k_2h_2) + B_2\cos(k_2h_2)\right] = 0, \\ \bar{c}_{66}k_1B_1 + e_{26}C_1 = \bar{\mu}k_2B_2, \\ \bar{\mu}k_2B_2 = K\left(A_2 - A_1\right), \\ \frac{e_{26}}{\varepsilon_{22}}A_1 + D_1 = -V_0. \end{cases} \tag{14}$$

From Eq. (14), we can derive the exact expressions of the undetermined coefficients as follows:

$$A_2 = \frac{2V_0}{\Delta},\ A_1 = P_1A_2,\ B_1 = P_2A_2,\ C_1 = P_3A_2,\ D_1 = -\frac{e_{26}}{\varepsilon_{22}}P_1A_2 - V_0,\ B_2 = \tan(k_2h_2)\,A_2 \tag{15}$$

where

$$\Delta = \frac{e_{26}}{\varepsilon_{22}}\left[P_1\cos(k_1h_1) - P_1 - P_2\sin(k_1h_1)\right] - P_3h_1, \tag{16.1}$$

$$P_1 = 1 - \frac{\bar{\mu}}{K}k_2\tan(k_2h_2), \tag{16.2}$$

$$P_2 = \frac{\bar{\mu}k_2\tan(k_2h_2) + \bar{c}_{66}k_1P_1\sin(k_1h_1)}{\bar{c}_{66}k_1\left[1 - \cos(k_1h_1)\right]}, \tag{16.3}$$

$$P_3 = -\frac{\bar{c}_{66}k_1\left[P_2\cos(k_1h_1) + P_1\sin(k_1h_1)\right]}{e_{26}}. \tag{16.4}$$

When $\Delta = 0$, the frequency equation of the thickness-shear mode in the QCM with zero initial voltage ($V_0 = 0$), which is related to the free vibration, is obtained as follows:

$$\begin{aligned} &k_1\left[1 - \cos(k_1h_1)\right]\left[1 - \frac{\bar{\mu}}{K}k_2\tan(k_2h_2)\right]\left\{k_1h_1\sin(k_1h_1) - \frac{e_{26}^2}{\bar{c}_{66}\varepsilon_{22}}\left[1 - \cos(k_1h_1)\right]\right\} \\ &+\left[k_1\sin(k_1h_1)\left[1 - \frac{\bar{\mu}}{K}k_2\tan(k_2h_2)\right] + \frac{\bar{\mu}}{\bar{c}_{66}}k_2\tan(k_2h_2)\right]\times \\ &\left\{k_1h_1\cos(k_1h_1) - \frac{e_{26}^2}{\bar{c}_{66}\varepsilon_{22}}\sin(k_1h_1)\right\} = 0. \end{aligned} \tag{17}$$

For the sake of convenience, a dimensionless interface parameter $\Gamma = \frac{c_{66}}{Kh_1}$ has been introduced. When $\Gamma \to +\infty$, the two layers are not attached, and as $\Gamma \to 0$, the two layers are attached perfectly.

3 Results and discussion

In this study, the characteristics of both the free and forced vibrations of QCM are studied. Polymethyl methacrylate (PMMA) is selected as the viscoelastic mass layer to investigate the effects of interface parameter and viscosity coefficient on the vibration frequency and admittance of QCM. The material constants of PMMA [25,26] and AT-cut quartz crystal [21,27] are listed in the "Appendix." The thickness of the quartz crystal plate (h_1) is fixed to be 0.5 mm.

3.1 Free vibration analysis

Equation (17) is a transcendental equation, in which the resonance frequency cannot be expressed with an explicit expression. Muller's method [28], which is an extension of the secant method, can be employed if the three initial values are properly selected for the convergence of the algorithm. However, Muller's method cannot be easily applied to our problem because the resonance frequency is unknown when the viscoelastic mass layer is very thin. Nevertheless, the initial resonance frequency can be obtained from the forced vibration analysis, as discussed in the next section.

Figure 2 shows the relationship between the resonance frequency (f) and thickness ratio ($\beta = h_2/h_1$) under different conditions. When $\beta = 0$, the frequency is constant and equals 3.3117 MHz, which is the resonance frequency of a blank quartz crystal plate with two electrodes. This validates the accuracy of the numerical calculations of this study. The calculated results obtained from Sauerbrey's equation [2,29] are also plotted in Fig. 2 for comparison. As can be seen, when β varies between 0 and 0.02, the results calculated using Eq. (17) are in accordance with those obtained with Sauerbrey's equation. Namely, Sauerbrey's equation is applicable if the viscoelastic mass layer is sufficiently thin. However, when the thickness of the mass layer is larger than 2% of the quartz plate thickness, i.e., $\beta > 0.02$, the effects of the interface parameter and viscosity coefficient on the resonance frequency become increasingly obvious, and the non-proportional relation between the resonance frequency and thickness ratio is increasingly evident. Therefore, Sauerbrey's equation ($\Delta f = -f_0^{3/2}\sqrt{\rho_L \eta_L}/\sqrt{\pi \rho_Q \mu_Q}$) in [2,29] cannot be used to exactly calculate the resonance frequency of the QCM when the mass layer is thick. To describe the effects of an additional mass layer on the performance of QCMs more accurately, the interaction between the layer and the AT-cut crystal plate and the viscoelasticity of the mass layer must be included in the analysis.

To further study the effects of interface parameter and viscosity coefficient, the frequency shift $\Delta f = f - f_0$ can be defined according to [20]. Here, f_0 is the resonance frequency of the blank quartz crystal plate with two electrodes, and $f_0 = 3.3117$ MHz in this study. Figures 3 and 4 show the variation of frequency shift (Δf) with the interface parameter (Γ) and viscosity coefficient (η), respectively. We fixed $\beta = 0.1$; therefore, Δf

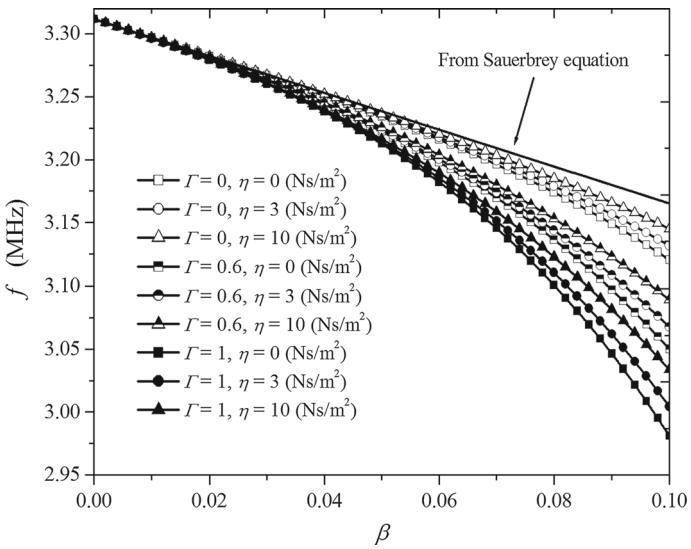

Fig. 2 Relationship between the resonance frequency and thickness ratio of the viscoelastic mass layer to the quartz plate

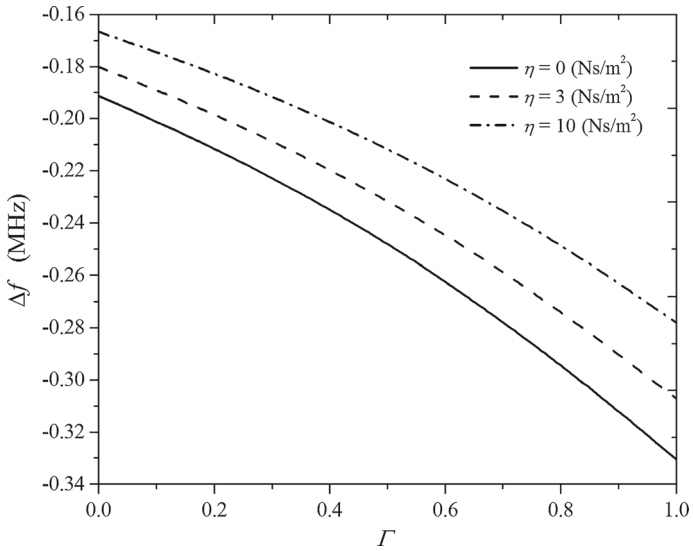

Fig. 3 Relationship between the frequency shift and the interface parameter

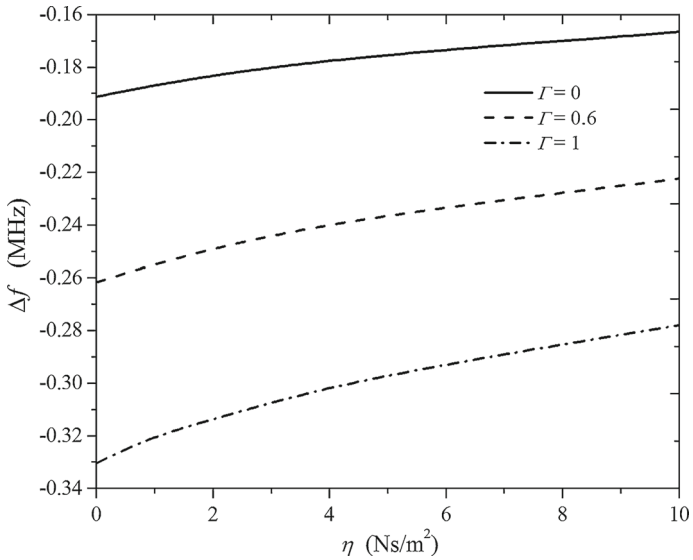

Fig. 4 Relationship between the frequency shift and the viscosity coefficient

is not equal to zero when $\Gamma = 0$ and $\eta = 0$. Some conclusions can be drawn from Figs. 3 and 4. Firstly, both Γ and η have a significant effect on Δf. Secondly, the absolute value of Δf increases as Γ increases because the stiffness of the whole structure decreases. As η increases, the absolute value of Δf decreases, because the elastic constant of the mass layer increases when η increases, which increases the stiffness of the whole structure.

The displacement and stress distributions along the thickness of the QCM under various conditions are illustrated in Figs. 5 and 6, respectively. The displacement and stress components have divided the maximum value when $\eta = 0$. In Fig. 5, we can see that the maximum displacement occurs at the surface of the viscoelastic mass layer, whereas the vibration near the middle plane of the crystal is approximately zero. However, the stress distribution is opposite. The maximum amplitude occurs at the middle plane of the crystal plate. When $y/h_1 = -1$ and $y/h_1 = 0.1$, the traction is free, which is given by Eq. (11). It should be noted that the displacement at the weak interface, i.e., $y/h_1 = 0$, is discontinuous owing to the application of boundary condition Eq. (13). Moreover, the amplitudes of displacement and stress decrease as the viscosity coefficient increases because the damping effect which will lead to energy loss becomes more significant with increasing viscosity coefficient.

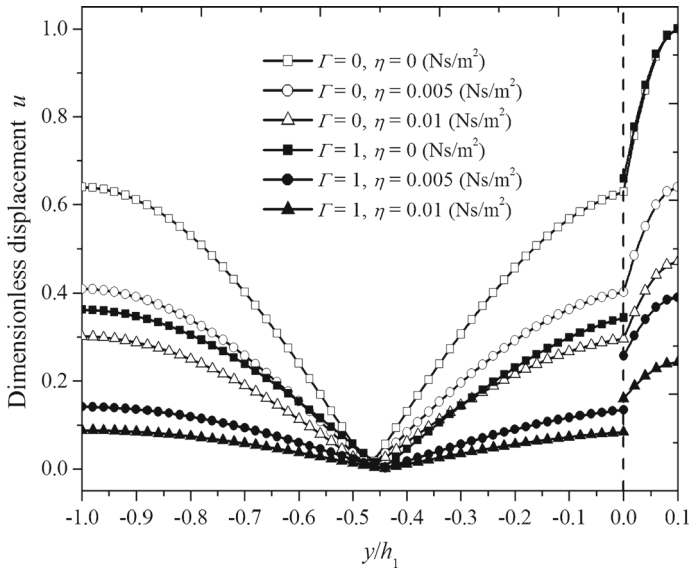

Fig. 5 Dimensionless displacement distribution along the thickness of QCM under different conditions

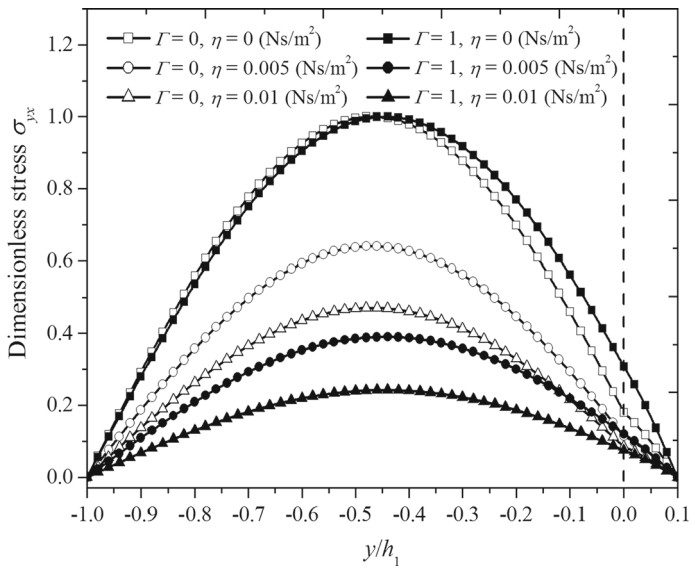

Fig. 6 Dimensionless stress distribution along the thickness of QCM under different conditions

3.2 Forced vibration analysis

In this section, forced vibration is discussed in detail for the case of $V_0 = 1$ V. Figures 7 and 8 show the effect of the interface parameter on the amplitude and phase of the admittance of the QCM, respectively, with $\eta = 0$ and $\beta = 0.1$. The admittance reaches the maximum at the resonance frequency. Moreover, it should be noted that the admittance amplitude is not zero at other frequencies. For instance, in the case of $\Gamma = 0$, the amplitude of admittance is 0.05234 S at a resonance frequency of $f = 3.12044$ MHz. When the frequency $f = 3.12723$ MHz, this value is only 0.00002 S. As the interface parameter increases, the plots of the admittance magnitude and corresponding phase exhibit a shift of the resonance peak toward a lower frequency as expected. The bandwidth of admittance at the resonant frequency is so narrow that the magnitude of admittance is very sensitivity to the step of the external frequency near the resonance frequency. Hence, the maximum value of admittance at resonances in the present contribution cannot be captured exactly. On the other hand, from numerical simulation, the admittance magnitude reaches its maximum when the

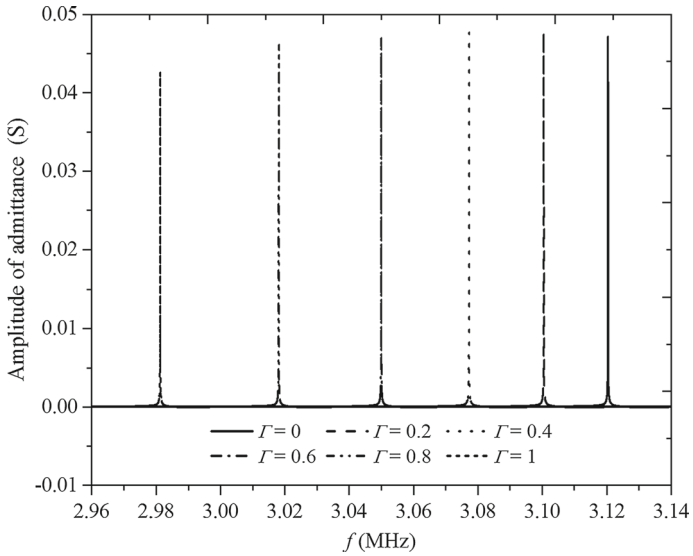

Fig. 7 Effect of interface parameter on the amplitude of admittance of the QCM when $\eta = 0$ and $\beta = 0.1$

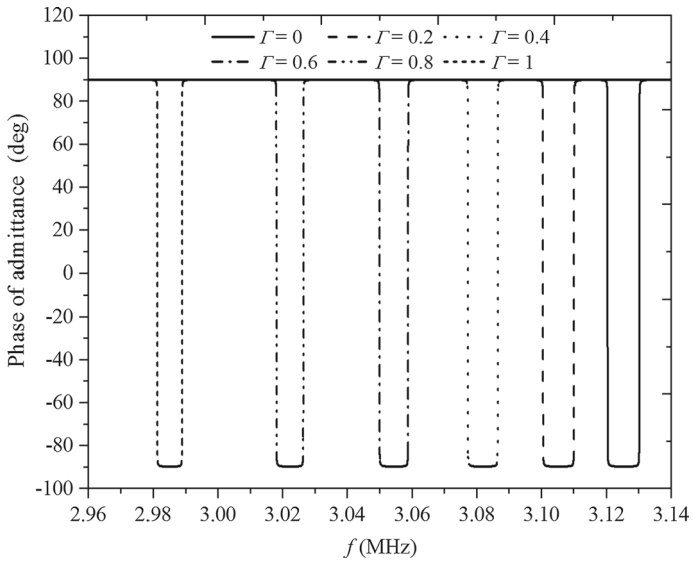

Fig. 8 Effect of interface parameter on the phase of admittance of the QCM when $\eta = 0$ and $\beta = 0.1$

corresponding phase angle first approaches zero. This phenomenon is the same as that of the unperturbed QCM [16].

The amplitude and phase distributions of the admittance of the QCM for some selected viscosities when the interface is perfectly bonded are shown in Figs. 9 and 10, respectively. As can be seen from Fig. 9, the resonant peak at $\eta = 0$ is much higher than those for other viscosity coefficients. As the viscosity coefficient increases, the resonant peak becomes smaller, and the bandwidth increases as more energy has been dissipated. Correspondingly, the mechanical quality factor of QCM has been reduced. For the case of antiresonance (the amplitude of the admittance reaches minimum at the antiresonant frequency), the antiresonant peak increases when the viscosity coefficient increases. As the viscosity coefficient increases, the phase of admittance becomes less sharp (Fig. 10). When the viscosity coefficient is sufficiently large, for instance, if η is larger than 5 $\mathrm{Ns/m^2}$, the phase of admittance is always larger than zero. It should be noted that at this time, i.e., the viscous coefficient is adequately large, the mass layer takes on more liquid-like properties. This phenomenon is very important for excitation within an oscillator [30,31]. However, the corresponding phase of admittance is still sensitive to viscosity variations. In general, we have studied the effects of imperfect interface and viscoelasticity of an

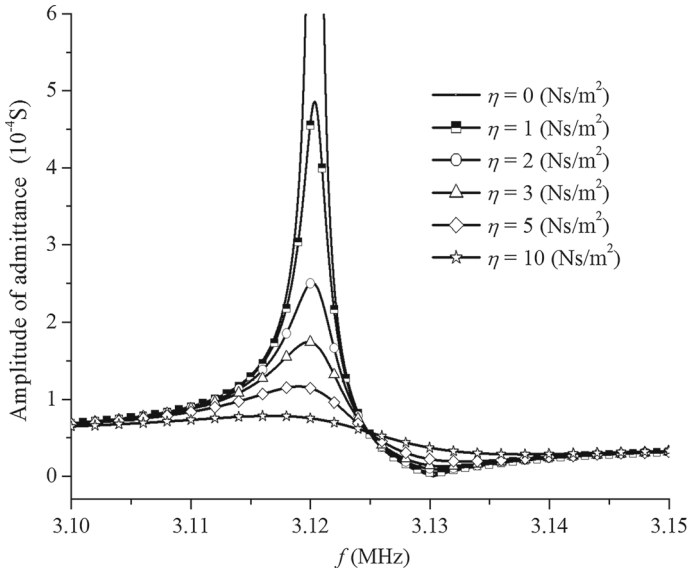

Fig. 9 Amplitude distribution of admittance of the QCM for some selected viscosities when $\Gamma = 0$ and $\beta = 0.1$

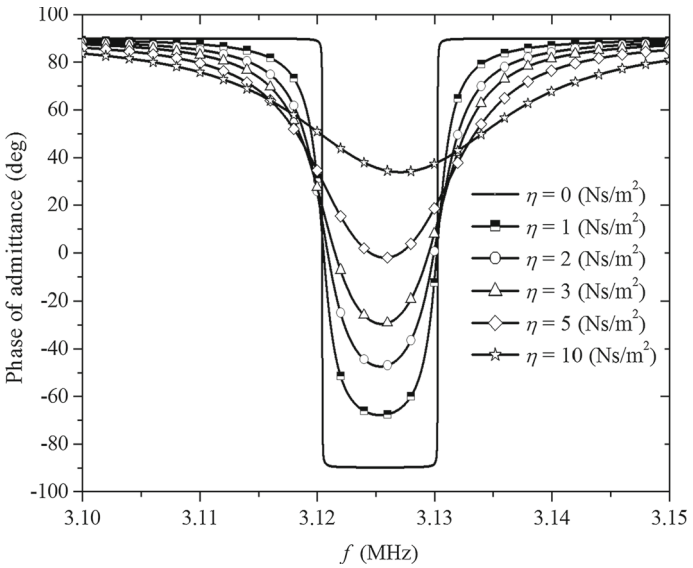

Fig. 10 Phase distribution of admittance of the QCM for some selected viscosities when $\Gamma = 0$ and $\beta = 0.1$

additional mass layer on QCM theoretically. Furthermore, the corresponding experimental investigations will be carried out in the future.

4 Conclusions

In this study, a detailed quantitative investigation has been conducted on the influence of the interface parameter and viscosity coefficient on the resonance frequency and admittance of QCMs. Muller's method is employed to solve the complex resonant frequency equation. The main conclusions can be summarized as follows:

(i) The non-proportional relation between the resonance frequency and thickness of the mass layer becomes obvious when the thickness of the mass layer is larger than 2% of the quartz plate thickness. The resonance frequency decreases as the interface parameter Γ increases from 0 to 1, while the resonance frequency increases when the viscosity coefficient η increases from 0 to 10 Ns/m^2.

(ii) With the interface parameter increasing, the admittance magnitude and the corresponding phase exhibit a corresponding shift of the resonance peak toward a lower frequency. As the viscosity coefficient increases, the resonant peak of the admittance becomes smaller and the bandwidth increases. When the viscosity coefficient η is larger than 5 Ns/m^2, the phase of admittance is always larger than zero.

The results obtained in the paper can provide a theoretical guidance for expanding the applications of QCMs attached to viscoelastic mass layers and developing high-performance chemical sensors and biosensors.

Acknowledgements The authors gratefully acknowledge the financial support provided by the National Natural Science Foundation of China (Nos. 31470908, 11672223, and 11472123) and the National 111 Project of China (No. B06024).

Appendix

Material constants of AT-cut quartz:
$c_{66} = 29.01 \times 10^9$ N/m^2, $e_{26} = -0.095$ C/m^2, $\varepsilon_{22} = 39.82 \times 10^{-12}$ C/Vm,
$\rho_1 = 2649$ kg/m^3, $\eta_q = 8.376 \times 10^{-3}$ Ns/m^2, $S = 0.2984$ cm^2.
Material constants of PMMA:
$\mu = 1.43 \times 10^9$ N/m^2, $\rho_2 = 1180$ kg/m^3.

References

1. Liu, N., Yang, J.S., Chen, W.Q.: Effect of a mass layer with gradually varying thickness on a quartz crystal microbalance. IEEE Sens. J. **11**(8), 1635–1639 (2011)
2. Sauerbrey, G.Z.: Use of quartz vibrator for weighing thin films on a microbalance. Z. Phys. **155**(2), 206–222 (1959). (**in German**)
3. Steen, C., Boersma, F., Ballegooyen, E.C.: The influence of mass loading outside the electrode area on the resonant frequencies of a quartz-crystal microbalance. J. Appl. Phys. **48**(8), 3201–3205 (1977)
4. Kong, Y.P., Liu, J.X., He, H.J., Yang, J.S.: Effects of mass layer dimension on a finite quartz crystal microbalance. Acta Mech. **222**(1–2), 103–113 (2011)
5. Josse, F., Lee, Y., Martin, S.J., Cernosek, R.W.: Analysis of the radial dependence of mass sensitivity for modified-electrode quartz crystal resonators. Anal. Chem. **70**(2), 237–247 (1998)
6. Lu, F., Lee, H.P., Lim, S.P.: Quartz crystal microbalance with rigid mass partially attached on electrode surfaces. Sens. Actuators A **112**(2–3), 203–210 (2004)
7. Li, Q., Gu, Y., Wang, N.F.: Free vibration analysis of a new polymer quartz piezoelectric crystal sensor applied to identify chinese liquors. Int. J. Appl. Mech. **9**(1), 1750015 (2017)
8. Hempel, U., Lucklum, R., Hauptmann, P.R., EerNisse, E.P., Puccio, D., Diaz, R.F.: Quartz crystal resonator sensors under lateral field excitation-a theoretical and experimental analysis. Meas. Sci. Technol. **19**(5), 055201 (2008)
9. Lucklum, R., Hauptmann, P.: Determination of polymer shear modulus with quartz crystal resonators. Faraday Discuss. **107**, 123–140 (1997)
10. Marx, K.A.: Quartz crystal microbalance: a useful tool for studying thin polymer films and complex biomolecular systems at the solution-surface interface. Biomacromolecules **4**(5), 1099–1120 (2003)
11. Kanazawa, K.K., Gordon, J.G.: Frequency of a quartz microbalance in contact with liquid. Anal. Chem. **57**(8), 1770–1771 (1985)
12. Kanazawa, K.K.: Mechanical behaviour of films on the quartz microbalance. Faraday Discuss. **107**, 77–90 (1997)
13. Sun, J.B., Du, J.K., Yang, J.S., Wang, J.: Shear-horizontal waves in a rotated Y-cut quartz plate in contact with a viscous fluid. Ultrasonics **52**(1), 133–137 (2012)
14. Arnau, A., Jimenez, Y., Sogorb, T.: An extended Butterworth–Van Dyke model for quartz crystal microbalance applications in viscoelastic fluid media. IEEE Trans. Ultrason. Ferroelectr. Freq. Control **48**(5), 1367–1382 (2001)
15. Suh, Y.K., Kim, B.C., Kim, Y.H.: Determination of viscoelastic property in polyethylene crystallization using a quartz crystal resonator. Sensors **9**(12), 9544–9558 (2009)
16. Martin, S.J., Granstaff, V.E., Frye, G.C.: Characterization of a quartz crystal microbalance with simultaneous mass and liquid loading. Anal. Chem. **63**(20), 2272–2281 (1991)
17. Vig, J.R., Ballato, A.: Comments on the effects of nonuniform mass loading on a quartz crystal microbalance. IEEE Trans. Ultrason. Ferroelectr. Freq. Control **45**(5), 1123–1124 (1998)
18. Chen, Y.Y., Du, J.K., Wang, J., Yang, J.S.: Shear-horizontal waves in a rotated Y-cut quartz plate with an imperfectly bonded mass layer. IEEE Trans. Ultrason. Ferroelectr. Freq. Control **58**(3), 616–622 (2011)
19. Li, P., Jin, F.: Effect of an imperfect interface in a quartz crystal microbalance for detecting the properties of an additional porous layer. J. Appl. Phys. **115**(5), 054502 (2014)
20. Liu, B., Jiang, Q., Yang, J.S.: Frequency shifts in a quartz plate piezoelectric resonator in contact with a viscous fluid under a separated electrode. Int. J. Appl. Electrom. **35**(3), 177–187 (2011)
21. Lu, F., Lee, H.P., Lim, S.P.: Mechanical description of interfacial slips for quartz crystal microbalances with viscoelastic liquid loading. Smart Mater. Struct. **12**(6), 881–888 (2003)

22. Nwankwo, E., Durning, C.J.: Impedance analysis of thickness-shear mode quartz crystal resonators in contact with linear viscoelastic media. Rev. Sci. Instrum. **69**(6), 2375–2384 (1998)
23. Nagy, P.B.: Ultrasonic classification of imperfect interfaces. J. Nondestruct. Eval. **11**(3–4), 127–139 (1992)
24. Lavrentyev, A.I., Rokhlin, S.I.: Ultrasonic spectroscopy of imperfect contact interfaces between a layer and two solids. J. Acoust. Soc. Am. **103**(2), 657–664 (1998)
25. Kielczynski, P.: Attenuation of Love waves in low-loss media. J. Appl. Phys. **82**(2), 5932–5937 (1997)
26. Liu, J.S., Wang, L.J., Lu, Y.Y., He, S.T.: Properties of Love waves in a piezoelectric layered structure with a viscoelastic guiding layer. Smart Mater. Struct. **22**(12), 125034 (2013)
27. Yang, J.S.: An Introduction to the Theory of Piezoelectricity. Springer, Boston (2005)
28. McMullan, C., Mehta, H., Gizeli, E., Lowe, C.R.: Modelling of the mass sensitivity of the Love wave device in the presence of a viscous liquid. J. Phys. D Appl. Phys. **33**(23), 3053–3059 (2000)
29. Itoh, A., Ichihashi, M.: A frequency of the quartz crystal microbalance (QCM) that is not affected by the viscosity of a liquid. Meas. Sci. Technol. **19**(7), 075205 (2008)
30. Zhang, H.F., Bao, Y.Y.: Sensitivity analysis of multi-layered *c*-axis inclined zigzag zinc oxide thin-film resonators as viscosity sensors. IEEE Trans. Ultrason. Ferroelectr. Freq. Control **61**(3), 525–534 (2014)
31. Qin, L.F., Chen, Q.M., Cheng, H.B., Chen, Q., Li, J.F., Wang, Q.M.: Viscosity sensor using ZnO and AlN thin film bulk acoustic resonators with tilted polar *c*-axis orientations. J. Appl. Phys. **110**(9), 094511 (2011)